THE JOURNAL OF BIOLOGICAL CHEMISTRY
Vol. 278, No. 30, Issue of July 25, pp. 27876–27887, 2003

Printed in U.S.A.

Electron Transfer in Cyanobacterial Photosystem I

II. DETERMINATION OF FORWARD ELECTRON TRANSFER RATES OF SITE-DIRECTED MUTANTS IN A PUTATIVE ELECTRON TRANSFER PATHWAY FROM A_0 THROUGH A_1 TO F_X*

Received for publication, March 24, 2003, and in revised form, April 23, 2003
Published, JBC Papers in Press, April 29, 2003, DOI 10.1074/jbc.M302965200

Wu Xu‡, Parag R. Chitnis‡, Alfia Valieva§, Art van der Est§, Klaus Brettel¶, Mariana Guergova-Kuras‖, Yulia N. Pushkar, Stephan G. Zech**, Dietmar Stehlik**, Gaozhong Shen‡‡, Boris Zybailov‡‡, and John H. Golbeck‡‡§§**

*From the ‡Department of Biochemistry, Biophysics, and Molecular Biology, Iowa State University, Ames, Iowa 50011, the §Department of Chemistry, Brock University, St. Catharines, Ontario L2S 3A1, Canada, the ¶Service de Bioénergétique, CEA and URA 2096 CNRS, CEA/Saclay, 91191 Gif-sur-Yvette, Cedex, France, the ‖Institut de Biologie Physico-Chimique, Centre National de la Recherche Scientifique, UPR 1261, 13 Rue Pierre et Marie Curie, 75005 Paris, France, the **Fachbereich Physik, Freie Universität, Berlin, Arnimallee 14, D14195 Berlin, Germany, and the ‡‡Department of Biochemistry and Molecular Biology, Penn State University, University Park, Pennsylvania 16802*

The directionality of electron transfer in Photosystem I (PS I) is investigated using site-directed mutations in the phylloquinone (Q_K) and F_X binding regions of *Synnechocystis* sp. PCC 6803. The kinetics of forward electron transfer from the secondary acceptor A_1 (phylloquinone) were measured in mutants using time-resolved optical difference spectroscopy and transient EPR spectroscopy. In whole cells and PS I complexes of the wild-type both techniques reveal a major, slow kinetic component of $\tau \approx 300$ ns while optical data resolve an additional minor kinetic component of $\tau \approx 10$ ns. Whole cells and PS I complexes from the $W697F_{PsaA}$ and $S692C_{PsaA}$ mutants show a significant slowing of the slow kinetic component, whereas the $W677F_{PsaB}$ and $S672C_{PsaB}$ mutants show a less significant slowing of the fast kinetic component. Transient EPR measurements at 260 K show that the slow phase is ~3 times slower than at room temperature. Simulations of the early time behavior of the spin polarization pattern of $P_{700}{}^+A_1{}^-$, in which the decay rate of the pattern is assumed to be negligibly small, reproduce the observed EPR spectra at 260 K during the first 100 ns following laser excitation. Thus any spin polarization from $P_{700}{}^+F_X{}^-$ in this time window is very weak. From this it is concluded that the relative amplitude of the fast phase is negligible at 260 K or its rate is much less temperature-dependent than that of the slow component. Together, the results demonstrate that the slow kinetic phase results from electron transfer from Q_K-A to F_X and that this accounts for at least 70% of the electrons. Although the assignment of the fast kinetic phase remains uncertain, it is not strongly temperature dependent and it represents a minor fraction of the electrons being transferred. All of the results point toward asymmetry in electron transfer, and indicate that forward transfer in cyanobacterial PS I is predominantly along the PsaA branch.

The pathway of light-induced electron transfer among symmetrically placed electron transfer cofactors has been a long standing issue in the study of photosynthetic reaction centers (RCs).[1] Although RCs show considerable diversity between various organisms, all consist of a protein dimer with two branches of cofactors that extend across the membrane from a "special pair" of chlorophyll molecules on the donor side to a pair of quinones on the acceptor side. The whole arrangement has pseudo-C_2 symmetry, however, differences in the amino acid sequences of the two proteins and/or positions and structures of the cofactors break the symmetry significantly in all heterodimeric RCs. In Type II RCs, quinones function as the terminal electron acceptors, and electron transfer is known to be highly asymmetric and strongly biased toward one branch (referred to as the A-branch). One apparent reason for this asymmetry is the fact that the quinone acceptor in the B-branch, Q_B, functions as a mobile electron carrier, and electron transfer down the A-branch stabilizes the electron while the Q_B site undergoes a structural reorganization needed to accept an electron (1). In Type I RCs, there are no known mobile quinones, and both branches converge at the iron-sulfur cluster F_X on the stromal side of the membrane. The electron is further transferred to the F_A and F_B iron-sulfur clusters, which function as the terminal electron acceptors. Because of these differences, the directionality of electron transfer in Type I RCs cannot be inferred from knowledge of Type II RCs.

Unlike in the bacterial RC, the two branches in Photosystem I (PS I) are difficult, if not impossible, to distinguish spectroscopically. As discussed in the previous paper (2), the use of point mutants and time-resolved EPR and optical spectroscopy allows this issue to be addressed in PS I. The initial electron transfer steps are difficult to observe because the trapping of the excitation from the antenna masks these early events. In contrast, the subsequent electron transfer from phylloquinone (A_1) to the iron-sulfur center F_X is easily observed and provides a convenient way to study the kinetics and pathway of electron transfer.

Early time-resolved optical studies of electron transfer from $A_1{}^-$ to F_X appeared to be contradictory, with kinetics from UV absorbance changes attributed to $A_1{}^-$ reoxidation reported to

* This work was supported by National Science Foundation Grants MCB-0117079 (to J. H. G.) and MCB-0078264 (to P. R. C.), Deutsche Forschungsgemeinschaft Grants SFB 498 and TP A3 (to D. S.) and grants from the Natural Sciences and Engineering Research Council, The Canada Foundation for Innovation, and The Ontario Innovation Trust (to A. v. d. E.). The costs of publication of this article were defrayed in part by the payment of page charges. This article must therefore be hereby marked "*advertisement*" in accordance with 18 U.S.C. Section 1734 solely to indicate this fact.

§§ To whom correspondence should be addressed. Fax: 814-863-7024; E-mail: JHG5@psu.edu.

[1] The abbreviations used are: RC, reaction center; PS, photosystem; EPR, electron paramagnetic resonance; Chl, chlorophyll; phylloquinone, 2-methyl-3-phytyl-1,4-naphthoquinone or 2-methyl-3-(3,7,11,15-tetramethyl-2-hexadecenyl)-1,4-naphthalenedione.

have a $t_{1/2}$ of 15 ns in PS I particles isolated from spinach (3) and 200 ns in PS I particles isolated from *Synechococcus* sp (4), whereas transient EPR data on PS I particles from *Synechococcus* sp. and spinach chloroplasts both gave a value of $\tau = 260$ ns ($t_{1/2} = 180$ ns) (5, 6). Later studies using so-called PS I-β particles from spinach showed a biphasic decay attributed to A_1^- oxidation with $t_{1/2}$ of 25 and 250 ns, and relative amplitudes of 65 and 35%, respectively (7). Both kinetic phases were attributed to electron transfer from A_1^- to F_X. Studies at faster time scales with PS I particles from *Synechocystis* sp. PCC 6803 also showed an additional kinetic phase attributed to A_1^- oxidation with a $t_{1/2}$ of 10 ns (8). Although the faster of the two kinetic phases cannot be resolved directly by transient EPR, changes in its relative amplitude are reflected in the observed spin polarization (9, 10), which is sensitive to the spin dynamics of short-lived precursor states with lifetimes as short as 500 ps.

Recently, this influence of the fast kinetic phase on the spin polarization patterns was investigated (9), and it was concluded that the amplitude of the fast phase in whole cells and PS I particles of cyanobacteria could account for at most ~20% of the total amplitude, whereas the transient EPR spectra of PS I particles isolated from spinach and *Chlamydomonas rheinhardtii* show a much larger influence (9). Moreover, the ratio of the fast to slow kinetic phases is not constant between different preparations; rather, PS I particles isolated from spinach show a diminished amplitude of the optically detected 25-ns kinetic phase when isolated using less harsh conditions, down to 30% in a particle prepared without detergent (7), whereas transient EPR suggests at most a very small contribution from the fast kinetic phase in spinach chloroplasts and cyanobacterial whole cells (6, 9, 10).

In contrast, recent optical studies of whole cells of *C. reinhardtii* (11) showed biphasic kinetics attributed to the reoxidation of A_1^- with $t_{1/2}$ of 18 ns and $t_{1/2}$ of 160 ns and of nearly equal amplitude. Hence, it appears that the fast kinetic phase is a property inherent to PS I but the ratio of the amplitudes of the fast and slow kinetic phases is species-dependent and sensitive to environmental conditions such as the presence of the detergent. Moreover, the sensitivity to detergent isolation is much higher in eukaryotic PS I compared with cyanobacterial PS I. Whereas the biphasic kinetics observed in the near UV are now generally thought to result from electron transfer from A_1^- to F_X, the origin of the biphasic behavior remains controversial (see Ref. 12 for review). Sétif and Brettel (7) suggested that the redox potentials of A_1 and F_X are close and that the fast kinetic phase reflects the establishment of a redox equilibrium between A_1 and F_X. This proposal was made prior to detailed knowledge about the pseudo C_2 symmetry of PS I, and therefore presupposes a unidirectional pathway of electron transfer. Joliot and Joliot (11) suggested that the biphasic kinetics could come about from either two conformational states that differ by the reoxidation rate of A_1^- or two phylloquinones that correspond to the two branches of the PS I heterodimer involved in electron transfer. The former presupposes unidirectional electron transfer and the latter presupposes bidirectional electron transfer.

The latter idea arose when the model of PS I based on the 6-Å crystal structure (13) showed the presence of a 2-fold axis of symmetry similar to the pseudo 2-fold axis of symmetry in the purple bacterial RC. The atomic resolution structure based on the 2.5-Å electron density map (14, 15) shows that the position of the electron transfer cofactors and the identity and positions of nearby amino acids are highly similar on the PsaA side and the PsaB side polypeptides. In particular, the phylloquinones on the PsaA side and the PsaB side are located in similar environments that consist of: (i) a H-bond between a backbone Leu and the stromal-facing carbonyl group of phylloquinone in the ortho position relative to the phytyl tail, (ii) a $\pi-\pi$ interaction with a Trp, and (iii) an apparent lack of a H-bond to the other phylloquinone carbonyl group in the meta position relative to the phytyl tail. One significant break in symmetry is in the P_{700} chlorophyll a'/a special pair; the chlorophyll a' has three H-bonds to PsaA side amino acids, whereas there are no H-bonds to the chlorophyll a on the PsaB side. Other significant symmetry breaks are also found further down the electron transfer chain in the high resolution structure (15).

The extent to which the two quinones are active in the electron transport chain, the origin of the biphasic kinetics of A_1^- reoxidation, and the role that the structural features of the binding site play in determining the electron transfer kinetics are all unresolved issues. In this paper, we report EPR and optical kinetic studies of mutants in and around the quinone binding sites of PS I. The premise of these experiments is that a change in the environment of the quinone should lead to a change in its redox potential, which, in turn, should translate to a change in the forward kinetics of electron transfer from the quinone to the iron-sulfur clusters. A network of H-bonded residues extends from the Met axial ligand of A_0 through A_1 to F_X. The residues involved in this network are thus candidates for point mutations, which are expected to influence the rate of forward electron transfer.

In the preceding paper (2), we showed that the point mutations $W697F_{PsaA}$, $W677F_{PsaB}$, $S692C_{PsaA}$, $S672C_{PsaB}$, $R694A_{PsaA}$, and $R674A_{PsaB}$ cause only subtle structural and electronic changes so that they act as suitable markers for following the pathway of electron transfer. As discussed in the preceding paper (2), the $W697F_{PsaA}$, $W677F_{PsaB}$, $S692C_{PsaA}$, and $S672C_{PsaB}$, mutants affect the quinone binding sites and we expect only electron transfer in the branch containing the mutation to be affected. The $R694A_{PsaA}$ and $R674A_{PsaB}$ mutants on the other hand may affect both branches because each is involved in a salt bridge from the **jk**-surface loop to $Gly^{572}{}_{PsaB}$ ($Gly^{585}{}_{PsaA}$) in the respective F_X binding loop (16). In other words, this residue ties together the region of the quinone with that of the iron-sulfur cluster. Mutations of these residues should disrupt this arrangement and would be expected to cause a change in the properties of F_X. The results presented in this paper address the issue of directionality and biphasic kinetics and can be interpreted to show that in *Synechocystis* sp. PCC 6803, the majority of electrons proceed along PsaA side cofactors in PS I. Whereas we cannot rule out the participation of PsaB side cofactors in PS I electron transfer, we place an upper limit on the fraction of electrons taking this pathway.

MATERIALS AND METHODS

Mutants and Photosystem I Complexes—The mutant strains containing the $W697F_{PsaA}$, $W677F_{PsaB}$, $S692C_{PsaA}$, $S672C_{PsaB}$, $R694A_{PsaA}$, and $R674A_{PsaB}$ substitutions have been described previously (2). Isolation of membranes and purification of PS I complexes was performed according to previously published procedures (2).

Flash-induced Transient Absorption Spectroscopy in the Near UV/Blue Region—Flash-induced absorbance changes of isolated PS I complexes were measured with a time resolution of about 2 ns with a set-up described previously (17) using 300-ps pulses of about 300 nJ/cm^2 at 532 nm for excitation (repetition rate, 1 Hz) and the relatively flat top of a 50-μs Xe flash as measuring light. Stock solutions of PS I complexes were diluted in a buffer containing 50 mM Tris, pH 8.3, 10 mM sodium ascorbate, and 500 μM 2,6-dichloroindophenol, to a final Chl concentration of typically 60 and 150 μM for measurements at 380 and 480 nm, respectively. The optical path length for the measuring light was 2 mm. Between 1024 and 4096 transients were averaged for each sample and wavelength to improve the signal-to-noise ratio. A Marquardt least squares algorithm program was used for fitting of the absorbance

change transients to a multiexponential decay. Time zero was defined as the midpoint of the rising edge of the transient, and fitting was started 2.5 ns after time zero.

Flash-induced absorbance changes in whole cells were measured with an optical setup described previously (18). Cells were centrifuged and resuspended in 20 mM Tris at pH 8.2 in the presence of 5% Ficoll. Dichlorodimethylurea (20 μM) and 2 mM hydroxylamine were added to inactivate Photosystem II and 20 μM carbonyl cyanide *p*-trifluoromethoxyphenylhydrazone was added to prevent accumulation of transmembrane potential.

X-band Transient EPR Spectroscopy at Room Temperature—Transient EPR experiments at room temperature were carried out using a modified Bruker ESP 200 spectrometer equipped with a home-built, broadband amplifier (bandwidth >500 MHz) for direct detection experiments. Light excitation was provided by a Continuum YAG/OPO laser system operating at 680 or 532 nm and 10 Hz. The EPR signals were digitized using a LeCroy LT322 500 MHz digital oscilloscope and transferred to a PC for storage and analysis. The samples were measured using a flat cell and a Bruker rectangular resonator and contained 1 mM sodium ascorbate and 50 μM phenazine methosulfate as external redox mediators. The response time of the system is governed by the bandwidth of the resonator and is estimated to be ~50 ns; the decay of the spin polarization limits the accessible time range to times shorter than a few microseconds. Complete time/field data sets were collected and analyzed to determine the lifetimes of the species and their decay-associated spectra. To ensure that the isolation procedure does not influence the kinetics or polarization patterns, transient EPR measurements of whole cells and isolated particles from wild-type *Synechocystis* sp. PCC 6803 were compared. The observed spin polarization patterns (not shown) and kinetic traces are identical demonstrating that the isolation of the particles has no effect on the kinetics.

X-band Transient EPR Spectroscopy at 260 K—X-band transient EPR experiments on frozen solutions at 260 K were carried out using a Bruker ER046 XK-T microwave bridge equipped with a Flexline dielectric resonator (6) and an Oxford liquid helium gas-flow cryostat. The loaded Q-value for this dielectric ring resonator was about $Q = 3000$, equivalent to a rise time of $\tau_r = Q/(2\pi \times \nu_{mw}) \approx 50$ ns. The samples were illuminated using a Spectra Physics Nd-YAG/MOPO laser system operating at 10 Hz and contained 1 mM sodium ascorbate and 50 μM phenazine methosulfate.

RESULTS

Our main effort focuses on applying a set of complementary spectroscopic techniques to characterize transient charge separated states in a comparative study of the influence of mutations near the A_1 binding site. We begin with studies of optical absorbance changes in the near UV/blue in both whole cells and in PS I complexes and continue with transient EPR spectroscopy.

Time-resolved Optical Measurements in Whole Cells and Isolated PS I Complexes—The advantage of studying kinetic processes in whole cells is that there is no potential damage to the acceptor cofactors as a result of detergent solubilization of the thylakoid membranes. The disadvantage is that the cells are actively growing and dividing, and PS I complexes may be present in a number of developmental states, including those undergoing assembly and those undergoing degradation. To minimize any potential for heterogeneity because of turnover and to reduce effects of background absorption and competing photoprocesses in larger antenna systems, studies were performed on whole cells and purified on PS I complexes. Ideally, the kinetic results should match in both studies.

The flash-induced difference spectrum of A_1^-/A_1 shows a broad absorption increase between 340 and 400 nm (4, 19). Measurements on PS I complexes were made at 380 and 480 nm, an absorption band in the visible spectrum that reflects the reduction of A_1. For technical reasons, measurements were performed at 390 and 400 nm on whole cells. Fig. 1 depicts the decay of the relative flash-induced absorbance change at 400 nm on a logarithmic time scale in whole cells of the wild-type in comparison with the $W697F_{PsaA}$ (*top*) and $W677F_{PsaB}$ (*bottom*) mutants. Table I summarizes the lifetimes and relative amplitudes as obtained from a fit of the data to the sum of a fast and slow

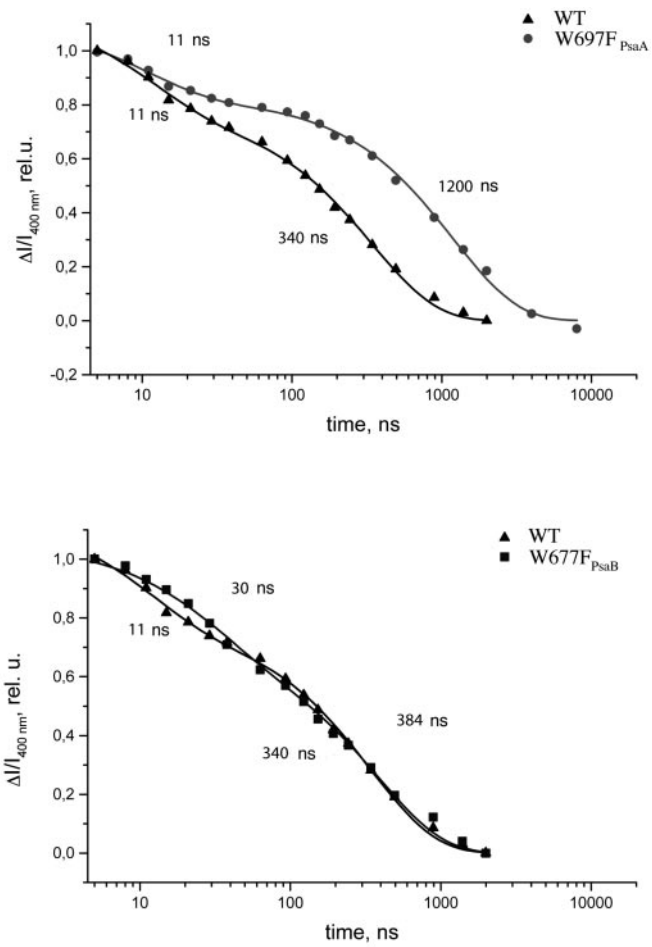

FIG. 1. **Kinetics of flash-induced absorbance changes at 400 nm in whole cells from the $W697F_{PsaA}$ (*top*) and $W677F_{PsaB}$ (*bottom*) mutants and compared with the wild-type at room temperature.** The experimental points are shown as discrete *points* and *lines* represent the best fit of the two exponential components with the lifetimes indicated on the figure. The data are plotted in relative ΔI/I units against a logarithmic time scale.

kinetic phase. At detection wavelengths of 390 and 400 nm, two kinetic phases are found in the wild type with similar time constants of $\tau = 10$ and $\tau = 300$ ns in an amplitude ratio of about 2:3. In the PsaA side mutant $W697F_{PsaA}$ the lifetime of the slow kinetic phase is increased by a factor of about 4 but the lifetime of the fast kinetic phase is relatively unchanged. In the corresponding (symmetric) PsaB side mutant $W677F_{PsaB}$ the lifetime of the slow kinetic phase is not changed significantly at either wavelength (see Table I) but the lifetime of the fast kinetic phase is increased by a factor of about 2.7 (see Fig. 1, *top*).

Examples of flash-induced absorption changes at 380 nm measured in isolated PS I complexes with a time resolution of about 2 ns are shown in Fig. 2. All samples studied showed an instrument limited rise of absorption (including the formation of A_1^- (4, 19)). As in whole cells, the subsequent decay of the signal (attributed to electron transfer from A_1^- to the iron-sulfur clusters (3, 4, 7, 8, 11)) was affected by the mutations. The wild-type signal (Fig. 2) could be well fitted with two exponential decay phases of $\tau = 10.6$ and $\tau = 240$ ns at an amplitude ratio of about 1:3 (see Table II), in line with a previous report (8).[2] Compared with the measurements on

[2] A slight bleaching present at the end of the depicted time scale is presumably from the state $P_{700}^+(F_A/F_B)^-$ and/or a small number of antenna chlorophyll triplets.

TABLE I

Kinetic analysis of flash-induced absorbance changes attributed to A_1^- reoxidation in whole cells

The fitted values are lifetimes (τ) and relative amplitudes taken from a two-exponential fit to the data at either 390 or 400 nm; the error in τ is estimated to be about 20%.

	390 nm				400 nm			
	τ	Relative amplitude	τ	Relative amplitude	τ	Relative amplitude	τ	Relative amplitude
	ns		*ns*		*ns*		*ns*	
WT	10	0.40	300	0.60	11	0.34	340	0.66
$W697F_{PsaA}$	11	0.42	1280	0.58	12	0.27	1200	0.73
$W677F_{PsaB}$	27	0.36	400	0.64	29	0.38	380	0.62
$S692C_{PsaA}$[a]	15	0.35	1340	0.65	14	0.38	1140	0.62
$S672C_{PsaB}$	13	0.38	210	0.62	15	0.41	240	0.59
$R674A_{PsaB}$	11	0.30	1300	0.70	12	0.32	1300	0.68

[a] In this mutant, a fast kinetic component (τ = 30 ns) was observed at 430 nm. The fast decrease of the signal may suggest that some PS I complexes undergo a charge recombination from $P_{700}^+A_0^-$.

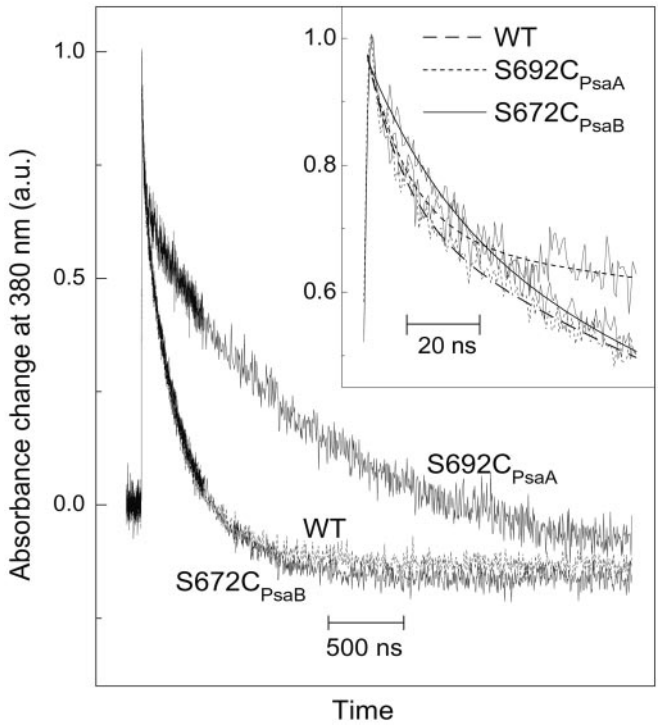

FIG. 2. **Kinetics of flash-induced absorbance changes at 380 nm in isolated PS I complexes from wild-type (*WT*), $S692C_{PsaA}$, and $S672C_{PsaB}$ at room temperature.** The *inset* shows the same traces on an expanded scale, together with the best biexponential fits (see Table II; *dashed line*, wild-type; *dotted line*, $S692C_{PsaA}$; *solid line*, $S672C_{PsaB}$). The signals were arbitrarily normalized for the ease of comparison. The maximal amplitudes correspond to absorbance changes of 6.7×10^{-4} for the wild-type (optical density of the sample at 679 nm, A_{679} = 0.76), 8.9×10^{-4} for $S692C_{PsaA}$ (A_{679} = 1.02), and 8.7×10^{-4} for $S672C_{PsaB}$ (A_{679} = 0.98).

whole cells from the wild type at 390 and 400 nm (see Table I), the lifetimes of the two phases are rather similar, but the relative amplitude of the faster phase appears to be smaller in isolated PS I (but only at 380 nm, not at 480 nm). For the mutants $W697F_{PsaA}$ and $W677F_{PsaB}$, the kinetics in isolated PS I complexes followed the same trends as in whole cells, *i.e.* the slower phase alone was slowed in the PsaA side mutant, whereas the faster phase alone was slowed in the PsaB side mutant. The relative amplitudes of the two phases were not significantly affected by these mutations (data not shown; see Table II for fit results). Similar results were observed in mutants of *C. reinhardtii* (20), in which the mutation of Trp to Phe on PsaA increased the lifetime of the slow phase while the corresponding (symmetric) mutation on PsaB slowed down the fast phase.

The lifetimes and amplitudes as obtained from a fit of the data to a fast and slow kinetic phase in whole cells of the wild-type, $S692C_{PsaA}$, and $S672C_{PsaB}$ mutants are summarized in Table I. In the PsaA side mutant $S692C_{PsaA}$, the lifetime of the slow kinetic phase is increased by a factor of about 4, whereas within experimental error the lifetime of the fast kinetic phase does not appear to be lengthened. In the corresponding (symmetric) PsaB side mutant $S672C_{PsaB}$, the lifetime of the slow kinetic phase is not changed significantly at either wavelength (see Table I). Surprisingly, within experimental error the lifetime of the fast kinetic phase also does not appear to be lengthened at either detection wavelength. Note particularly that the large effect on the slow kinetic phase of the $S692C_{PsaA}$ mutant is not mirrored by that on the fast kinetic phase in the $S672C_{PsaB}$ mutant. However, because of the smaller number of data points that determine the fast kinetics phase and its relatively small amplitude the evaluated kinetic parameters are more reliable for the slow component than the fast component.

Consistent with the results on whole cells, isolated PS I from the mutant $S672C_{PsaA}$ showed a pronounced slowing of the slower phase and virtually no effect on the faster phase (Fig. 2). The fit results (Table II) appear to indicate some increase (compared with the wild type) of the relative amplitude of the fast phase. However, some evolution of the kinetics was observed upon prolonged experimentation with this sample (see Footnote a of Table II), so that the effect on the amplitude of the $S672C_{PsaA}$ mutation should be interpreted with caution. The corresponding PsaB side mutation $S672C_{PsaB}$ showed no significant effect on the slow phase, but there was an approximate 2-fold increase in the lifetime of the fast phase (Fig. 1). The latter observation deviates from the results on whole cells in which the same mutation in PsaB appeared to have less of an effect on the kinetics of A_1^- oxidation.

It has been shown previously (4, 19) that absorption changes associated with A_1^- can be observed around 480 nm, although the nature of this absorption band is not fully established (an electrochromic bandshift of a nearby carotenoid because of the negative charge on A_1^- has been suggested (4)). Fit results of 480 nm measurements on isolated PS I complexes from the wild type and the four mutants described above are also listed in Table II. In all cases, the mutation effects are similar to those observed at 380 nm, including some slowing of the faster phase in the $S672C_{PsaB}$ mutant. The changes in relative amplitudes differ at the two wavelengths and in all samples the relative amplitude of the faster phase is significantly higher at 480 nm compared with 380 nm. This is in line with previous reports comparing the absorbance difference spectra of the two

TABLE II
Kinetic analysis of flash-induced absorbance changes attributed to A_1^- reoxidation in isolated PS I complexes

	380 nm				480 nm			
	τ	Relative amplitude	τ	Relative amplitude	τ	Relative amplitude	τ	Relative amplitude
	ns		*ns*		*ns*		*ns*	
WT	11	0.25	240	0.75	9.8	0.39	230	0.61
$W697F_{PsaA}$	8.7	0.26	720	0.74	8.1	0.38	880	0.62
$W677F_{PsaB}$	32	0.24	260	0.76	23	0.41	260	0.59
$S692C_{PsaA}$[a]	12	0.29	1040	0.71	7.7	0.38	1330	0.62
$S672C_{PsaB}$	25	0.26	280	0.74	17	0.43	250	0.57

[a] A significant evolution of the kinetics during prolonged repetitive excitation was observed for this mutant. The data presented in the table result from accumulations of 2048 transients (380 nm) and 1024 transients (480 nm) measured with freshly prepared samples. For a sample that had received about 6000 excitation flashes, a biexponential fit of the 380-nm signal yielded lifetimes (relative amplitudes) of 22 (0.58) and 580 ns (0.42). A significantly better fit was obtained with three exponentials: 9.4 (0.38), 61 (0.30), and 830 ns (0.32). The error in τ is estimated to be 20%.

phases: when normalizing the spectra in the 380-nm band, the 480-nm band was more pronounced for the faster phase than for the slower phase (7, 8, 11).

Together the data show that for all mutations expected to influence electron transfer in the PsaA branch, the slow kinetic phase is slowed significantly. It is less clear whether such a trend holds for the fast kinetic phase. The measured lifetimes for the Trp mutants suggest that the fast phase is only affected by mutations on the PsaB branch. However, for the Ser mutants, mutations in the PsaB branch showed a significant slowing of the fast phase only in isolated PS I and not in whole cells, although the corresponding mutations in the PsaA branch consistently affect the slow phase in both types of samples.

Room Temperature Electron Spin-polarized EPR Signals at X-band—Fig. 3 compares spin-polarized EPR transients of wild-type PS I and the $W697F_{PsaA}$ (*left*) and $W677F_{PsaB}$ (*right*) mutants, respectively. The transients are taken at selected field positions as indicated in the spectra at the *top* of the figure. As the electron is transferred from A_1^- to F_X, the emission/absorption/emission (E/A/E) polarization pattern of $P_{700}^+A_1^-$ changes to one with net emission from P_{700}^+ in the $P_{700}^+(FeS)^-$ state where FeS is one of the iron-sulfur centers. We refer to these two spectra as the early spectrum ($P_{700}^+A_1^-$) and the late spectrum ($P_{700}^+(FeS)^-$). At field position **a**, only the A_1^- contribution to $P_{700}^+A_1^-$ is observed, so that the decay of the EPR signal at this field position reflects the forward electron transfer, provided that it is significantly faster than the decay of the spin polarization. At other field positions, contributions from both $P_{700}^+A_1^-$ and $P_{700}^+(FeS)^-$ occur. As is evident from the kinetic traces, the transients from the $W697F_{PsaA}$ mutant (Fig. 3, *left*) are significantly different from the wild-type and forward electron transfer is slower in this mutant. A fit of the data yields a lifetime for the electron transfer of $\tau = 640 \pm 50$ ns in the $W697F_{PsaA}$ mutant compared with $\tau = 240 \pm 50$ ns in the wild-type. In contrast, the transients and spectra from the $W677F_{PsaB}$ mutant are indistinguishable from wild-type PS I. Fig. 4 shows corresponding transients for the $S692C_{PsaA}$ and $S672C_{PsaB}$ mutants, which have similar kinetic behavior to the Trp mutants (Fig. 3) except that the effect of the PsaA mutation is even greater. A fit of the data set yields a lifetime of $\tau = 1290 \pm 50$ ns in the $S692C_{PsaA}$ mutant. Again, the PsaB mutant is indistinguishable from the wild type. Thus, consistent with the optical data, a slowing of the slow phase is observed as a result of the mutations in the PsaA-branch quinone binding site. The corresponding PsaB branch mutations do not cause any detectable change in the spin polarization.

Room temperature transients of the $R694A_{PsaA}$ and $R674A_{PsaB}$ mutants are shown in Fig. 5. Clearly the data from the two mutants are very similar. An analysis of the data sets in the forward electron transfer rate from A_1^- is slowed and yields almost identical values of $\tau = 640 \pm 50$ ns and $\tau = 680 \pm 50$ ns for the respective mutants. The optical absorbance changes in whole cells of the $R674A_{PsaB}$ mutant also show an increase in the lifetime of the slow phase (Table I) but the lifetime obtained is roughly a factor of two longer. The origin of this difference in the observed lifetimes is unclear but it may be related to temperature differences between the two experiments (see below). The fact that the slowing of the electron transfer rate obtained from the EPR experiments is the same for both the PsaA- and PsaB-branch mutants can be rationalized by making the reasonable assumption that the mutations primarily affect the redox potential of F_X (see "Discussion"). However, the optical data show no effect on the fast phase in the $R674A_{PsaB}$ mutant (see Table I). In addition, the $R694A_{PsaA}$ mutation leads to changes in the spin density on A_1^- as observed in low temperature electron nuclear double resonance and transient EPR experiments (see previous paper, Ref. 2). Hence it is likely that factors other than the redox potential of F_X are also influenced by mutation of these Arg residues.

The values of the optically determined lifetimes of the slow phase for the mutants shown in Tables I and II are in reasonable qualitative agreement with the values determined from the transient EPR experiments summarized in Table III. However, the whole cell experiments in Table I give lifetimes that are consistently longer. This is likely a result of a difference in "room temperature" between the experiments. Spin relaxation can also influence the lifetimes obtained from EPR transients; however, relaxation effects are microwave power dependent (6) and no significant dependence on the microwave power was found for the electron transfer lifetimes. Hence different temperatures are the more likely cause of the difference in the lifetimes determined optically and from EPR.

Both the optical and the transient EPR data show that the slow kinetic phase is associated with electron transfer along the PsaA branch. However, no clear influence from the fast kinetic phase observed optically is detectable in the EPR data. As discussed in Ref. 9 if the two phases correspond to two fractions in the sample with different rates of electron transfer from A_1^- to F_X, then both fractions contribute to the spin polarization observed for $P_{700}^+(FeS)^-$ and they are sensitive to both the relative magnitude of the two fractions and their lifetimes. In spinach samples known to contain a large fraction of fast electron transfer the influence of the fast phase is clearly evident (10) in the transient EPR data and it leads to a spectrum with net emission at early times. This raises the question of how large an effect is expected in the transient EPR data of the samples studied here based on the amplitudes and lifetimes

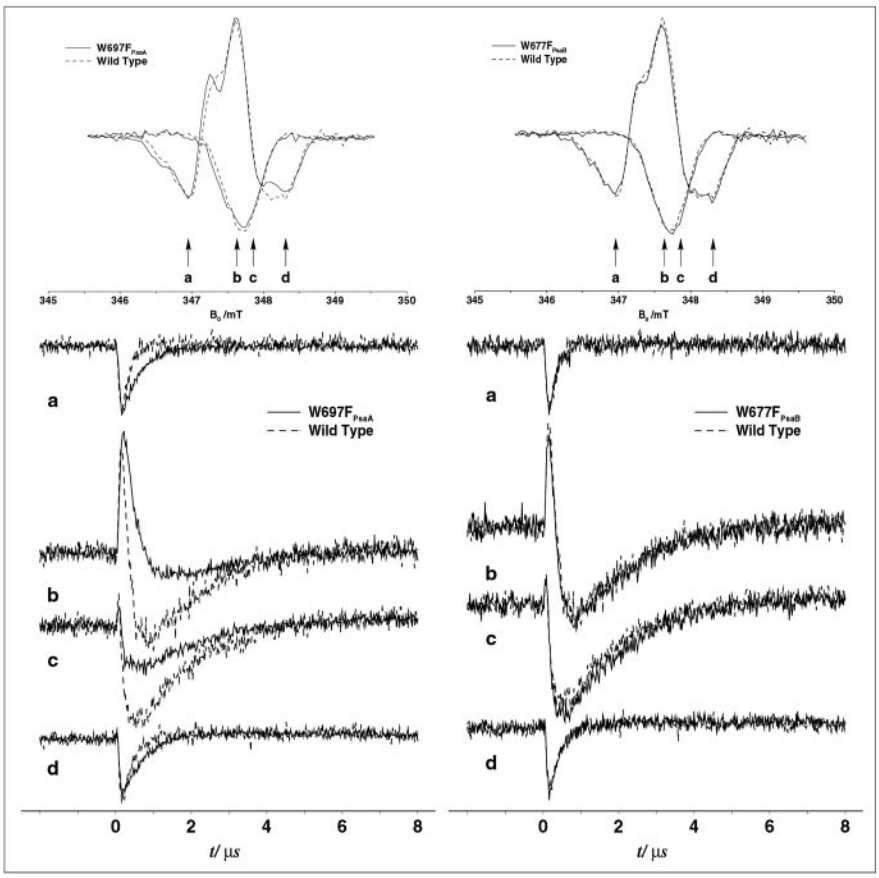

FIG. 3. **Room temperature transient EPR kinetic traces of PS I complexes from the W697F$_{PsaA}$ mutant (*left*) and the W677F$_{PsaB}$ mutant (*right*) compared with wild-type.** The field positions at which the transients were taken are indicated by the *arrows* labeled *a–d below* the spectra of $P_{700}^{+}A_1^{-}$ and $P_{700}^{+}(FeS)^{-}$ shown at the *top* of the figure. The early and late spectra have been obtained using the fitting procedure described in Ref. 6. The *solid curves* are from the mutants and the *dashed curves* are from wild-type PS I.

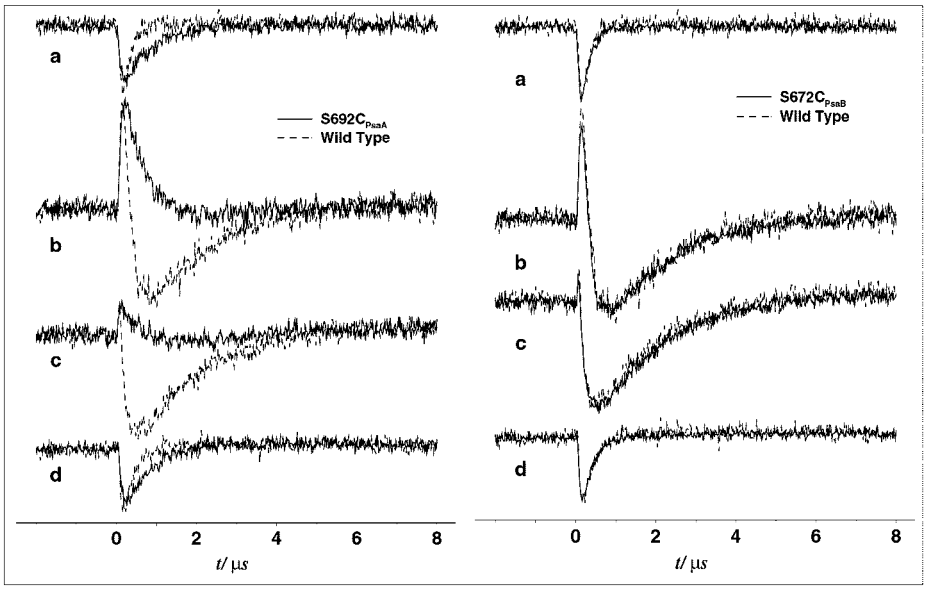

FIG. 4. **Room temperature transient EPR kinetics of whole cells of the S692C$_{PsaA}$ mutant (*left*) and S672C$_{PsaB}$ mutant (*right*) compared with wild-type PS I.** The field positions are the same as shown in Fig. 1. The *solid curves* are from the mutants and the *dashed curves* are from wild-type.

observed optically. Using the expressions discussed in Ref. 9 we estimate that the net polarization observed in the $P_{700}^{+}(FeS)^{-}$ state at X-band is zero if the lifetime of $P_{700}^{+}A_1^{-}$ is less than ~1 ns, is maximum if the lifetime of $P_{700}^{+}A_1^{-}$ is greater than ~100 ns, and most sensitive to changes in the rate of electron transfer when the lifetime of $P_{700}^{+}A_1^{-}$ is roughly 50 ns. Simulations of the spectra (not shown) indicate that for a lifetime of 10 ns for the fast phase, its contribution to the transient EPR signals would be within the signal to noise if it accounted for 20% or less of the reaction centers. Thus, the lifetimes and amplitudes of the fast phase given in Tables I and II are expected to produce signal contributions close to the detection limit of transient EPR and the changes in the lifetime of the fast phase occur in a time region (10 to 20 ns) in which the polarization is relatively insensitive to the lifetime.

EPR Studies of the Slowing of A_1^{-} Oxidation at 260 K—At temperatures between 260 and 300 K, charge separation between P_{700} and F_A/F_B remains reversible in wild-type PS I. The

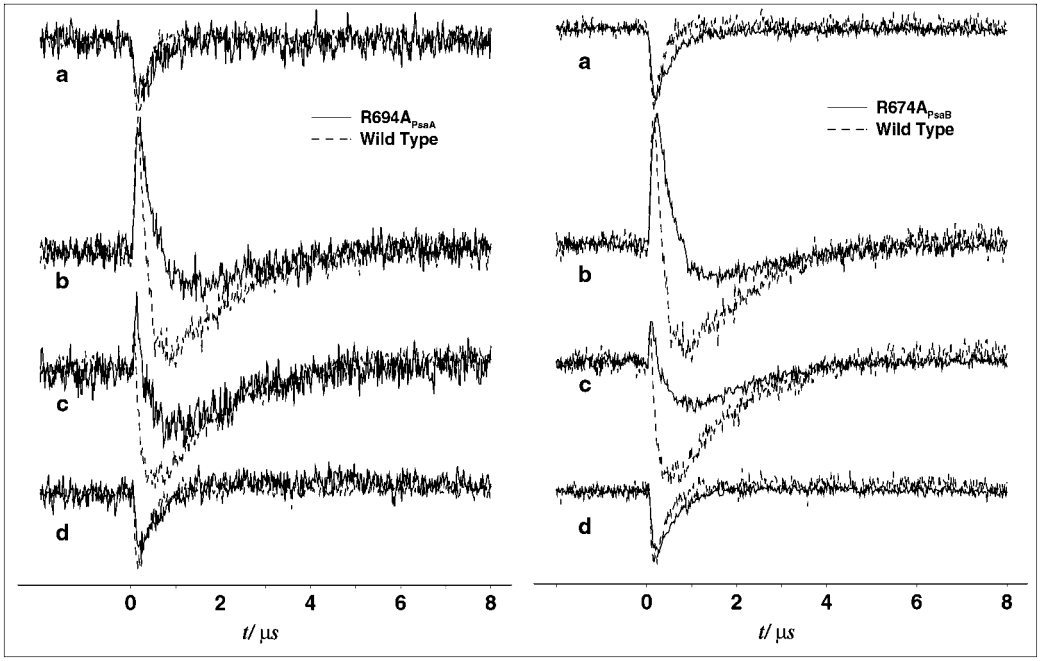

FIG. 5. **Room temperature transient EPR kinetics of the R694A$_{PsaA}$ mutant (*left*) and R674A$_{PsaB}$ mutants (*right*) compared with wild-type PS I.** The field positions are the same as shown in Fig. 1. The *solid curves* are from the mutants and the *dashed curves* are from wild-type.

TABLE III
Kinetic analysis of TR ESR spectra at 260 K and room temperature

	Room temperature[a]		260 K
	τ_{ET}	τ_{spin}[b]	τ_{ET}
	ns		*ns*
WT	240	1440	840 ± 50
W697F$_{PsaA}$	640	1360	1820 ± 100
W677F$_{PsaB}$	240	1670	840 ± 50
S692C$_{PsaA}$	1290	1350	3020 ± 100
S672C$_{PsaB}$	220	1500	840 ± 50
R694A$_{PsaA}$	640	1360	1000 ± 50
R674A$_{PsaB}$	680	1340	1100 ± 50

[a] Estimated error in all values ±20%.
[b] Effective relaxation times for microwave power 10 mW. At 260 K spin relaxation rates are too slow to be reliably evaluated.

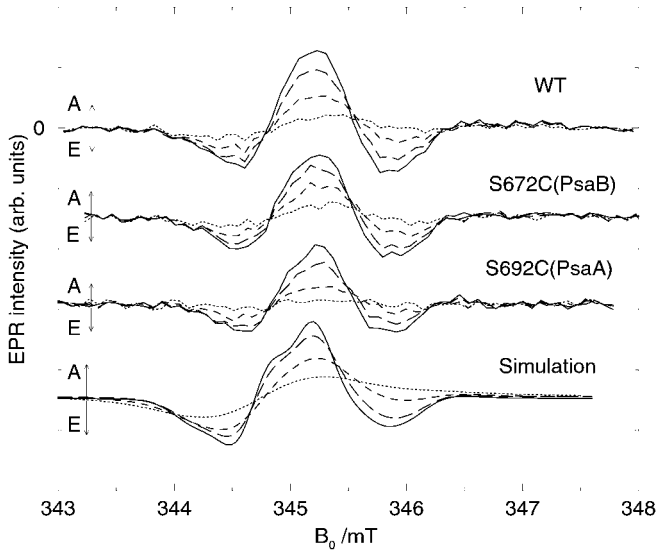

FIG. 6. **Early time development of the spin-polarized transient EPR spectra in PS I complexes of the wild-type, S672C$_{PsaB}$, and S692C$_{PsaA}$ mutants at 260 K compared with calculated spectra of the $P_{700}^{+}A_1^{-}$ state (see text for explanation).** The spectra are integrated in four successive 16-ns time windows starting 50 ns after the laser flash: 50–66 ns (*dotted line*), 66–82 ns (*short dashed line*), 82–98 ns (*long dashed line*), and 98–114 ns (*solid line*).

slow phase of forward electron transfer as measured by absorbance changes at 380 nm in PS I from *Synechococcus elongatus* (21) follows Arrhenius behavior with an activation energy of 220 ± 20 meV so that it is slowed by a factor of about 3 at 260 K compared with room temperature. If the fast and slow kinetic phases differ only in their activation energies then the fast component would have a lower activation energy and therefore a weaker temperature dependence. Transient EPR data taken below room temperature but above ~200 K allow the influence of the mutations on the activation energy to be investigated and may show signal contributions to the spin polarization from the fast phase, depending on how it changes with temperature. Spin polarization patterns and transients taken at 260 K are shown in Figs. 6 and 7, respectively, and the electron transfer lifetimes evaluated from the transient EPR data sets are given in Table III. The kinetics of A_1 oxidation are slowed by roughly the same factor of around 2–3 compared with room temperature for all of the samples. Thus, none of the mutations appears to have a large impact on the activation energy associated with the slow phase of electron transfer, and the kinetics of A_1^- oxidation in the W677F$_{PsaB}$ and S672C$_{PsaB}$ mutants remain identical to those of the wild-type at 260 K. The possible influence of the fast kinetic phase on the spin polarization patterns is investigated directly in Fig. 6, which shows early spectra in four successive 16-ns time windows for the wild-type and the S672C$_{PsaB}$ and S692C$_{PsaA}$ mutants. In general, the polarization patterns of spin-correlated radical pairs exhibit lifetime or Fourier broadening as well as coherence effects because of transient mutations, quantum beats, and envelope modulation (22–25). Coherence effects do not make significant contributions under our experimental conditions and Fourier broadening dominates the short time behavior at X-band. As is

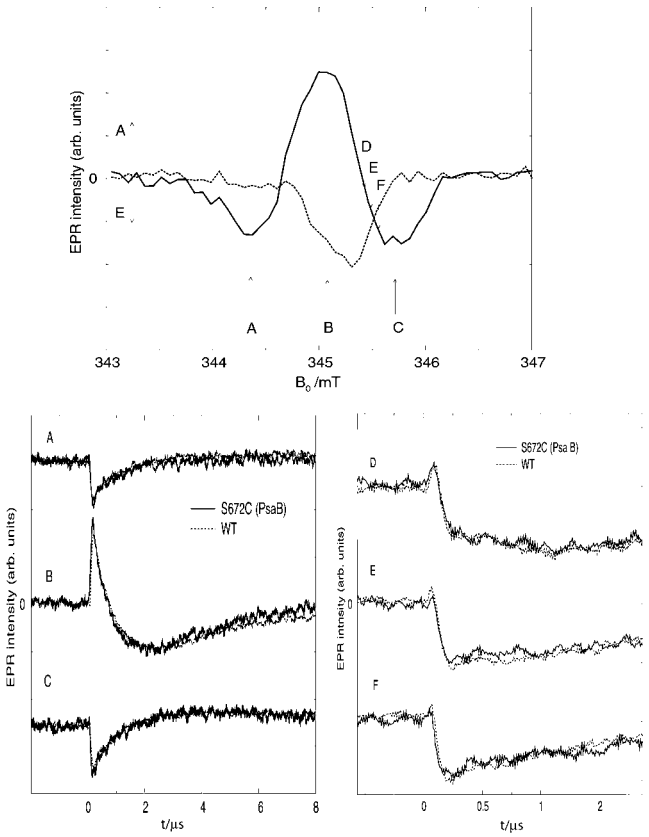

FIG. 7. **Transient EPR kinetic traces at selected magnetic field positions for the field positions (*bottom*) for the S672C$_{PsaB}$ mutant compared with wild-type PS I at 260 K.** The *arrows A–F* in the kinetically separated spectra indicate the field positions selected for the transients (*bottom*).

evident in Fig. 6, the broadening causes an up-field shift of the up-field zero-crossing of the E/A/E polarization pattern. This shift is very well reproduced in numerical simulations (Fig. 6, *bottom*) of the $P_{700}^{+}A_1^{-}$ spectrum based on the spin-correlated radical pair model (23, 26) in which the signal decay is assumed to be negligibly slow. Thus, it is clear that $P_{700}^{+}A_1^{-}$ dominates the early spectra. Moreover, within experimental error, the net polarization of the experimental spectra is zero. Thus, no evidence is found for spin polarization associated with $P_{700}^{+}(FeS)^{-}$ from the fast kinetic phase in the electron transfer between A_1^{-} and the iron-sulfur clusters.

This was also confirmed by the selected transients shown in Fig. 7 taken at 260 K for wild-type PS I and the S672C$_{PsaB}$ mutant. The transients at the maxima of the $P_{700}^{+}A_1^{-}$ spectrum (field positions A, B, and C) are analogous to those measured at room temperature (see Fig. 3) and do not exhibit any significant difference between the mutant and the wild type. The transients taken up-field of the zero-crossing point of the $P_{700}^{+}A_1^{-}$ spectrum (positions D, E, and F) demonstrate the influence of Fourier broadening by the short (<100 ns) initial, absorptive (positive) spike in transients D, E, and F generated by the shift of the zero-crossing point in the early spectra of Fig. 7. The spike at these field positions can only result from the $P_{700}^{+}A_1^{-}$ state. Any early contribution from the $P_{700}^{+}(FeS)^{-}$ state can only have an emissive (negative) amplitude. Because within experimental accuracy the spike does not change in amplitude between the wild-type and both mutants S672C$_{PsaB}$ and S692C$_{PsaA}$ (not shown), we conclude that the mutations do not cause a measurable change of the early signal for the time range >20 ns. If the fast kinetic phase were subject to the same activation process as the slow phase and if we extrapolate from the optically determined rates listed in Table II at room temperature, then the fast phase would slow to about 75 to 90 ns, which is within the time resolution of transient EPR. In addition, the spin polarization pattern of $P700^{+}$ A_1^{-}, as well as that of the subsequent $P_{700}^{+}(FeS)^{-}$ state, would be characteristically different as predicted from the theoretical description of sequentially populated radical pairs (27, 28). However, if the fast phase was activationless and its relative amplitude remained the same or similar to that found at room temperature, it would remain difficult to detect at 260 K. Thus, the transient EPR data suggest that either the activation energies of the two phases are considerably different or the amplitude of the fast phase becomes smaller at low temperature.

DISCUSSION

The results above show that mutations in the vicinity of the phylloquinones and F_X in PS I show a clear influence on the kinetics of electron transfer from A_1^{-} to F_X. Nevertheless, to interpret the data in terms of the directionality of electron transfer requires an assignment of the kinetic phases to electron transfer from a specific quinone to F_X. In a number of recent studies, it has been proposed that the electron transfer is bidirectional on the premise that the observed biphasic A_1^{-} oxidation kinetics represents electron transfer along the two branches of cofactors. However, some of the data presented here, particularly from transient EPR, raise questions about this assignment. Because this is such a crucial point in the analysis of our results, we will first summarize the existing data supporting bidirectional *versus* unidirectional electron transfer.

Evidence for Unidirectional Electron Transfer—Evidence favoring unidirectionality came first from continuous wave EPR experiments performed on deletion mutants of *Synechocystis* sp. PCC 6803. When wild-type PS I complexes are illuminated at 205 K in the presence of sodium hydrosulfite at pH 10.5, A_1^{-} is photoaccumulated within minutes. However, when PS I complexes from a PsaE/PsaF deletion mutant are illuminated under similar conditions, only A_0^{-} is photoaccumulated (29). The premise is that photoaccumulation of A_0^{-} can occur only when phylloquinone is doubly reduced; a necessary precondition for its appearance is that the semiquinone anion must be protonated prior to the second reduction step. The proton becomes available by the removal of PsaE/PsaF and the subsequent action of Triton X-100, which are proposed to open a water channel to the phylloquinone associated with the PsaA subunit. The logic behind the experiment is that if electron transfer were unidirectional, then there should have been either an all-or-none loss of the photoaccumulated A_1^{-} signal depending on which branch is active. However, if electron transfer were bidirectional, then there should have been a loss of that percentage of the photoaccumulated A_1^{-} signal associated with the slow phase. The total loss of photoaccumulated A_1^{-} and its replacement by A_0^{-} in the PsaE/PsaF mutant implies that electron transfer is unidirectional along PsaA subunit (29). This suggests that the mutation and the detergent alter the environment of the quinone on the PsaA side of PS I, perhaps by removing a chlorophyll molecule that would otherwise shield the quinone from the hydrophilic surroundings. A related issue is that it is very difficult to accumulate a second spin on the phylloquinone in PS I from *Synechococcus* sp. PCC 7002 (29) or *Synechocystis* sp. PCC 6803.[3] Were electron transfer to be bidirectional, then it might be expected that once the PsaA side quinone is photoaccumulated as A_1^{-}, then it should

[3] B. Zybailov and J. H. Golbeck, unpublished results.

be relatively straightforward to photoaccumulate the PsaB side quinone. Yet, A_1 becomes instead doubly reduced, and A_0^- is photoaccumulated (however, see Ref. 30 for experimental conditions under which a second quinone was reported to be photoaccumulated in PS I from *C. reinhardtii*).

The strength of the photoaccumulation protocol is that it subjects the sample to multiple turnovers, thereby providing a large number of opportunities for any given electron to be transferred through either potential pathway of cofactors. The weakness of this protocol is that the photoaccumulation of A_1^- is a largely kinetic trick that requires special conditions of prolonged illumination in the presence of a high mobility reductant at low temperature in a glassy solid. Its success rests largely on a favorable combination of kinetic rates, particularly on forward electron transfer between the sulfite ion and P_{700}^+ at that time when the reaction center is in the charge separated state P_{700}^+ and A_1^-. Normally this is a low probability event, given the rapid charge recombination between P_{700}^+ and A_1^-, but given enough time, it can succeed in trapping a large percentage of the reaction centers in the $P_{700}^+A_1^-$ state. Given that these forward and backward rates are not well characterized as a function of temperature, it is not possible to predict with any confidence the effect on the ability to photoaccumulate A_1^- when the kinetic constants are altered. Nevertheless, the photoaccumulation experiment was the first to show that electron transfer occurred through the phylloquinone associated with the PsaA subunit (29). Also, this study, as well as a number of site-directed mutation experiments in a prokaryotic cyanobacterium and a eukaryotic alga (see next section) have confirmed that the optically detected slow A_1^- oxidation kinetics is associated with electron transfer along the PsaA side as is the EPR-detected transient $P_{700}^+A_1^-$ state.

Evidence for Bidirectional Electron Transfer—Evidence favoring bidirectionality is based largely on time-resolved optical studies of site-directed mutants in *C. reinhardtii* (20). These studies involve changing the π-stacked Trp on either the PsaA or PsaB subunits, and the results are most easily explained if the source of the biphasic kinetics of A_1^- oxidation is assumed to be the result of electron transfer through the symmetrically located branches of cofactors in PS I (11). The premise of this experiment is that changing the environment of the quinone should alter the redox potential, which because of the Frank-Condon term in the Marcus equation, should result in a change in the rate of electron transfer. A Trp → Phe mutation on the PsaB side slowed the 18-ns fast kinetic phase to 97 ns, and a Trp → Phe mutation on the PsaA side slowed the 218-ns slow kinetic phase to 609 ns (20). Only the relative kinetics of electron transfer appeared to be changed, not the amplitudes of the two kinetic phases. This is an important checkpoint because, as a first approximation, the percentage of electrons that travel up the PsaA and PsaB sides are already decided prior to the arrival of the electron at the quinone, and only the lifetimes of electron transfer from A_1^- to F_X should be affected. This experiment provided experimental support for the hypothesis that the two kinetic phases represent electron transfer through the two branches of cofactors in PS I. An EPR study of the PsaA side Trp → Leu and Trp → His mutations in *C. reinhardtii* showed a change of the relative amplitudes of the biexponential (spin relaxation) decay of the out of phase electron spin-echo signal arising from the $P_{700}^+A_1^-$ radical pair (31). At this time, there are no results reported on the PsaB side mutants. Thus the evidence is still inconclusive and very indirect. The strength of the optical kinetic protocol is that if one accepts the principles of Occam's razor, the biphasic kinetics are most easily explained by electron transfer through both branches of cofactors. The weakness of this protocol is that a number of factors are capable of providing biphasic kinetics, including microheterogeneity along a given branch of cofactors, and there is a reasonable probability that a point mutation near a cofactor can have an effect on other cofactors. This can be seen in this study in the counterintuitive effect on the fast and slow kinetic phases in the Arg mutants.

Finally, a series of biochemical experiments have been reported in which one of the two phylloquinones could be extracted without influencing rates of steady-state forward electron transfer to $NADP^+$ (32), or methyl viologen (33), the backreaction kinetics from $[F_A/F_B]^-$ to P_{700}^+ (32) or the transfer of an electron to F_A at either room or cryogenic temperatures (33). The removal of the second quinone eliminated electron transfer to $NADP^+$ and resulted in a 20-ns backreaction from A_0^- to P_{700}^+ (32). The assumption is that the first extracted quinone was derived from one of the two chains of cofactors rather than representing the statistical removal of one-half of the quinones from each cofactor side. The implication is that either one side of electron transfer cofactors is inactive, or that when one side of cofactors is missing, electron transfer can occur entirely through the other side of cofactors at high efficiency.

Assignment of the Kinetic Phases of A_1^- Reoxidation—While it is difficult to reconcile the results of all these experiments in a single, integrated model, there is full experimental agreement on one point: the slow kinetic phase of electron transfer occurs on the quinone associated with the PsaA subunit in PS I complexes from the eukaryotic organism *C. reinhardtii* (20) and from the prokaryotic organism *Synechocystis* sp. PCC 6803 (this work), and this is the same quinone that is observed by EPR in photoaccumulation experiments (29) and in low temperature spin-polarized EPR and electron nuclear double resonance experiments (2, 34).

The assignment of the fast phase is more problematic. The absorption difference spectra associated with the two decay lifetimes (10 and 300 ns) in whole cells of *Synechocystis* sp. PCC 6803 are nearly identical (data not shown). In isolated PS I from the same organism, the spectra of the two phases were found to be very similar between 330 and 440 nm, but deviated significantly between 450 and 490 nm (8). This would suggest that the fast phase corresponds to an event similar to the one associated with the slow phase: an electron transfer from a phylloquinone to an iron-sulfur cluster. The optical kinetic data on the Trp → Phe mutants in whole cells and in PS I complexes show a trend in *Synechocystis* sp. PCC 6803 similar to that described in *C. reinhardtii* (20). In both organisms, the lifetime of the fast kinetic phase becomes longer when the mutation is made on the PsaB side, and the lifetime of the slow kinetic phase becomes longer when the mutation is made on the PsaA side. The rate constant and the relative amplitude of the absorbance change are similar in whole cells and in PS I complexes, implying that detergent isolation does not perturb the kinetics in this set of mutants. The optical and EPR kinetic data on the Ser → Cys mutants shows that the lifetime of the slow kinetic phase becomes longer in the PsaA side mutant and the effect is larger than that observed for the Trp → Phe, again consistent with the assignment of the slow phase to electron transfer in the PsaA branch. In contrast, it is not as evident that the lifetime of the fast kinetic phase becomes longer in the Ser → Cys PsaB side mutant. The discrepancy between the whole cells and the PS I particle data (see Tables I and II) may be a function of the precision of the measurement, but the slowing is most likely not as strong as that in the corresponding Trp → Phe mutant.

The optical kinetic data on the $R674A_{PsaB}$ mutant appears to be hard to reconcile with the assignment of the fast phase as

electron transfer in the PsaB branch. Despite the fact that the mutation is on the PsaB side of the reaction center between Q_K-B and F_X, the lifetime of the fast kinetic phase remains unaltered, whereas the lifetime of the slow kinetic phase increases significantly. As outlined in Ref. 16, $Arg^{694}{}_{PsaA}$ and $Arg^{674}{}_{PsaB}$ have an important role in the structural environment of both F_X and the respective phylloquinones Q_K-A and Q_K-B. The residue positions the flexible F_X binding loop of PsaA as it crosses over the PsaB region by a pair of hydrogen bonds. $Arg^{674}{}_{PsaB}$ may therefore interact with F_X via a salt bridge from the B-**jk** surface helix to $Gly^{585}{}_{PsaA}$. Thus, it is possible that the redox potential of F_X is decreased in this mutant and to the same extent in the C_2-symmetric $Arg^{694}{}_{PsaA}$ mutant. This hypothesis would explain the transient EPR data, which shows the same slowing of the (slow) kinetics in both the $Arg^{694}{}_{PsaA}$ and $Arg^{674}{}_{PsaB}$ mutants but is hard to reconcile with the fact that the fast phase is unaffected if the latter is associated with electron transfer along the PsaB branch. Alternately, if one assumes that the two kinetic phases are associated with different conformations of the protein rather than electron transfer through the two branches, then it is conceivable that the mutation has a more pronounced effect on one conformation than on the other. It is therefore possible that the changes in fast and slow kinetic phases are associated with electron transfer through only the PsaA side, and that the quinones associated with each kinetic phase are located in slightly different environments. However, the specific effect on the fast phase of mutations made in the close environment of the phylloquinone in the PsaB branch such as $W677F_{PsaB}$ is difficult to reconcile with this hypothesis. These data provide a good illustration of the difficulties associated with drawing conclusions from the changes induced by point mutations. Clearly, the effects of the mutations are likely to be more complex than just causing a small change in the local environment or the redox potential of a single cofactor. Thus, it is important to base conclusions on as much experimental data as possible.

We can summarize the above discussion as follows: all data are compatible with the assignment of the slow kinetic phase to electron transfer on the PsaA branch. In contrast, the assignment of the fast phase is less certain. The optical spectral characteristics reflect reoxidation of A_1^-, and some correlation with mutations in the PsaB branch exists. None of the data rule out electron transfer in the PsaB branch. However, the lack of independent confirmation by a second spectroscopic technique and the fact that the $R674A_{PsaB}$ mutation does not change the fast kinetic phase suggest that the assignment should be left as an open question at present.

Asymmetry of Electron Transfer—Having discussed the assignment of the kinetic phases, we now address the question of what fraction of the electrons follows each kinetic phase. Whereas it is clear that the optical data give a much better estimation of the fraction of fast kinetic phase, there appears to be a problem of consistency with the EPR data. Qualitatively, all of the data are consistent in showing that the slow kinetic phase accounts for the major fraction of all of the electrons. The relative amplitudes of the two phases obtained optically suggest that the slow phase accounts for roughly 70% of the electrons promoted by P_{700}. The EPR data, on the other hand, do not show any clear indication of the fast phase at either room temperature or at 260 K. As discussed above, the net polarization of P_{700}^+ generated by the fast kinetic phase lasts for many microseconds, so there is no issue of time resolution. However, if the lifetime of $P_{700}^+A_1^-$ is sufficiently short (10–20 ns) and the fraction of the fast component is sufficiently small, <20%, this polarization is likely to be difficult to detect underneath the much stronger polarization associated with the slow kinetic phase. For the room temperature data on wild-type PS I, comparison with simulated EPR spectra lead to the conclusion that at most ~20% of the reaction centers could have a 10-ns electron transfer time (28). A qualitative demonstration of the effect of the fast component suggested that for larger fractions, the amplitude ratio of the late and the early spectrum would be larger than observed. This ratio as extracted from the measured data depends on the deconvolution of the data for the instrument response and on the choice of the effective spin relaxation times of w_A and w_B of the pairs $P_{700}^+A_1^-$ and $P_{700}^+(FeS)^-$, respectively (see Equation 1 in Ref. 28). Although care has been taken to take these factors into account properly, some uncertainty exists in the values used. Specifically, w_A cannot not be determined experimentally in intact PS I. The value w_A measured in a sample lacking all three iron-sulfur centers is within error the same as w_B in intact samples measured under the same conditions (6, 28). Thus, here we have used the same relaxation rate for both radical pairs. However, the presence of the iron-sulfur clusters in intact sample could conceivably increase the relaxation rate and hence our value of w_A would be underestimated. Because the relative amplitude of the two signals depends on the factor $k + (w_A - w_B)$, an underestimation of w_A would lead to an underestimation of the amplitude of the late spectrum and hence to an underestimation of a potential fast phase of electron transfer. The values of w_A and w_B are strongly microwave power dependent, yet the decay of the $P_{700}^+A_1^-$ signal, which is governed by $k + w_A$, is independent of the microwave power in wild-type PS I (5) indicating that under the conditions used here, k is much larger than w_A. Thus, although it is possible that the two relaxation rates are not the same, it is unlikely that the uncertainty in $w_A - w_B$ is large enough to have any major influence on the relative amplitudes of the two signals in wild-type PS I. In the PsaA mutants, however, the values of k are considerably smaller and such effects could become important. Thus, although the relative amplitudes of the early and late transient EPR spectra do not give a clear indication of a fast component, they are not inconsistent with the fraction estimated from the optical results.

Another quantifiable criterion is the amount of net polarization in the early spectrum. For the pair $P_{700}^+A_1^-$, the net polarization is virtually zero because of the extremely short lifetime (~30 ps) of the precursor state of $P_{700}^+A_0^-$ (27). By contrast, $P_{700}^+(FeS)^-$ shows pronounced emissive polarization of P_{700}^+ (the contribution from $(FeS)^-$ is not visible because it relaxes very rapidly). Hence, the putative formation of $P_{700}^+F_X^-$ within about 10 ns in a fraction of the reaction centers should be visible as a net emission of the early EPR spectrum. In Fig. 4 of Ref. 27 a comparison of the simulated $P_{700}^+A_1^-$ spectrum with the early spectrum extracted by fitting the experimental kinetic traces of wild-type PS I is shown. From this comparison the early spectrum appears to be slightly emissive, however, it is not clear whether this is because the early and late spectra have not been separated completely by the fitting procedure or whether it is because of an additional signal contribution at early times. Therefore we have performed similar simulations (not shown) of the total EPR spectrum (*i.e.* the sum of all expected contributions) at several delay times following the laser flash and included various fractions of the reaction centers with a 10-ns phase. According to these simulations, 20–30% of a 10-ns phase is compatible with the net polarization of the measured room temperature transient EPR spectra in PS I from wild-type *Synechocystis* sp. PCC 6803.

It is of note that in spinach samples known to contain a large fraction of fast electron transfer the influence of the fast phase

is clearly evident (10) in the transient EPR data resulting in a spectrum with net emission at early times. Thus, there is no doubt that the presence of such a phase can be detected under the proper conditions. Because the strength of the net polarization increases with the lifetime of the precursor state, we had expected that the fast phase in our cyanobacterial samples would become more easily observable perhaps even directly by EPR by decreasing the temperature of the sample to 260 K. Yet, as shown above no clear indication of the fast phase was found. However, this is not surprising in light of a recent optical study on PS I from *Synechocystis* sp. PCC 6803 that showed that the rate of the fast phase was virtually independent of temperature and that its relative amplitude decreased from ~28% at room temperature to ~20% at 260 K (35). Three other observations at 260 K are surprising, however. (i) The early time behavior of the spin polarization could be simulated by a spin-correlated radical pair model with the assumption that only $P_{700}^{+}A_1^{-}$ contributed to the early spectra (see Fig. 6). (ii) Within experimental error, the net polarization of the spectra at early times was zero (Fig. 6). (iii) EPR transients of wild-type and $S692C_{PsaB}$ mutant were virtually identical (Fig. 7), although the fast phase as detected optically at room temperature was found to be about two times slower in isolated PS I from this mutant than in wild-type PS I.

All these observations can be most easily explained by the absence of a signal contribution from a fast phase of A_1^{-} reoxidation. The more difficult question, however, is whether this is because the phase is not present or whether the polarization associated with it is simply too weak to observe clearly. Because it is difficult to predict accurately whether 20% of a fast phase (with $\tau \approx 10$ ns in wild type and $\tau \approx 20$ ns in the $S692C_{PsaB}$ mutant) should produce effects that exceed the experimental error of the EPR experiments, this must be left as an open question at present.

CONCLUSIONS

There are two main points which all of the data support: (i) the slow phase represents electron transfer along the PsaA branch; and (ii) this phase represents the majority of electron transfer in cyanobacterial PS I. The reason for the discrepancy in the fast kinetic phase between the optical and EPR data is not obvious. It is conceivable that the spin polarization expected from the fraction of reaction centers associated with the fast phase is weak because of inefficient spin polarization or rapid relaxation. Whatever the case, it is clear that the large majority of electrons are transferred along the PsaA branch of cofactors and the forward electron transfer is biased in this direction.

These findings raise a number of important and interesting issues. First, the origin and functional significance of the asymmetry in the electron transfer remains unknown. Clearly, the asymmetry is determined in the initial charge separation step, however, the nature of P_{700}* is not known with certainty, and which of the chlorophylls acts as the initial acceptor is also unknown. It is generally assumed that this process is analogous to that in purple bacteria, for which asymmetric electron transfer is established. First, P* is localized on the special pair of chlorophylls, and the accessory chlorophyll acts as the acceptor. In PSI, the electronic structure and electrostatic environment of the P_{700} dimer are expected to be responsible for the asymmetry of electron transfer. Many of the properties of P_{700} display asymmetry; for example, the spin density distribution in P_{700}^{+} and the triplet excitation at low temperature. The most striking asymmetry, however, is the fact that the two chlorophylls are two different structural isomers, chlorophyll a' and chlorophyll a. Furthermore, the chlorophyll a' has three H-bonds to the PsaA side polypeptides, whereas chlorophyll a has no H-bonds to the PsaB side polypeptides. None of these properties gives a direct measure of the properties of P_{700}*, but they all suggest that the environment of the primary donor is conductive to electron transfer predominantly along one branch of acceptors.

Another issue is whether the asymmetry has any functional significance. Because both branches converge at F_X there is no reason why one branch should be favored over the other. However, forward electron transfer is not the only process in which the cofactors are involved. Specifically, the reaction center must also accommodate energy transfer to P_{700} and secondary electron donation from plastocyanin or cytochrome to P_{700}^{+}. Given, the apparent redundancy in the electron transfer chain it is conceivable that the asymmetry in the electron transfer is a consequence of optimization of energy transfer or secondary electron transfer.

Because there is considerable species variability in these secondary processes this raises the question of whether the asymmetry in the electron transfer might also be species dependent. Indeed, it is well known that biphasic electron transfer from A_1 to F_X in spinach is very sensitive to the isolation procedure, whereas such effects are not observed in cyanobacteria. Preliminary investigations of several plants and green algae indicate that this sensitivity also shows significant species dependence among eukaryotes. We are currently investigating these and other related issues to come to a more complete understanding of what factors influence the appearance of the slow and fast kinetic phases.

REFERENCES

1. Graige, M. S., Feher, G., and Okamura, M. Y. (1998) *Proc. Natl. Acad. Sci. U. S. A.* **95,** 11679–11684
2. Xu, W., Chitnis, P., Vaieva, A., van der Est, A., Pushkar, J., Teutloff, C., Krzystyniak, M., Zech, S., Bittl, R., Stehlik, D., Zybailov, B., Shen, G., and Golbeck, J. (2003) *J. Biol. Chem.* **278,** 27864–27875
3. Mathis, P., and Sétif, P. (1988) *FEBS Lett.* **237,** 65–68
4. Brettel, K. (1988) *FEBS Lett.* **239,** 93–98
5. Bock, C. H., van der Est, A. J., Brettel, K., and Stehlik, D. (1989) *FEBS Lett.* **247,** 91–96
6. van der Est, A., Bock, C., Golbeck, J., Brettel, K., Sétif, P., and Stehlik, D. (1994) *Biochemistry* **33,** 11789–11797
7. Sétif, P., and Brettel, K. (1993) *Biochemistry* **32,** 7846–7854
8. Brettel, K. (1998) in *Photosynthesis: Mechanisms and Effects* (Garag, G., ed) Vol. I, pp. 611–614, Kluwer Academic Publishers, Budapest, Hungary
9. Kandrashkin, Y. E., and van der Est, A. (2002) *RIKEN Rev.* **44,** 124–127
10. van der Est, A. (2001) *Biochim. Biophys. Acta* **1507,** 212–225
11. Joliot, P., and Joliot, A. (1999) *Biochemistry* **38,** 11130–11136
12. Brettel, K., and Leibl, W. (2001) *Biochim. Biophys. Acta* **1507,** 100–114
13. Krauß, N., Hinrichs, W., Witt, I., Fromme, P., Pritzkow, W., Dauter, Z., Betzel, C., Wilson, K. S., Witt, H. T., and Saenger, W. (1993) *Nature* **361,** 326–331
14. Jordan, P., Fromme, P., Witt, H. T., Klukas, O., Saenger, W., and Krauß, N. (2001) *Nature* **411,** 909–917
15. Fromme, P., Jordan, P., and Krauss, N. (2001) *Biochim. Biophys. Acta* **1507,** 5–31
16. Antonkine, M., Jordan, P., Fromme, P., Krauß, N., Golbeck, J., and Stehlik, D. (2003) *J. Mol. Biol.* **327,** 671–697
17. Brettel, K., Leibl, W., and Liebl, U. (1998) *Biochim. Biophys. Acta* **1363,** 175–181
18. Béal, D., Rappaport, F., and Joliot, P. (1999) *Rev. Sci. Instrum.* **70,** 202–207
19. Brettel, K., Sétif, P., and Mathis, P. (1986) *FEBS Lett.* **203,** 220–224
20. Guergova-Kuras, M., Boudreaux, B., Joliot, A., Joliot, P., and Redding, K. (2001) *Proc. Natl. Acad. Sci. U. S. A.* **98,** 4437–4442
21. Schlodder, E., Falkenberg, K., Gergeleit, M., and Brettel, K. (1998) *Biochemistry* **37,** 9466–9476
22. Salikhov, K. M., Bock, C. H., and Stehlik, D. (1990) *Appl. Magn. Res.* **1,** 195–211
23. Kothe, G., Weber, S., Bittl, R., Ohmes, E., Thurnauer, M. C., and Norris, J. R. (1991) *Chem. Phys. Lett.* **186,** 474–480
24. Salikhov, K. M., Zech, S., and Stehlik, D. (2002) *Mol. Phys.* **100,** 1311–1321
25. Bittl, R., van der Est, A., Kamlowski, A., Lubitz, W., and Stehlik, D. (1994) *Chem. Phys. Lett.* **226,** 349–358
26. Weber, S., Ohmes, E., Thurnauer, M. C., Norris, J. R., and Kothe, G. (1995) *Proc. Natl. Acad. Sci. U. S. A.* **92,** 7789–7793
27. Kandrashkin, E. M., Salikhov, K. M., van der Est, A., and Stehlik, D. (1998) *Appl. Magn. Reson.* **15,** 417–447
28. Kandrashkin, Y. E., Vollmann, W., Stehlik, D., Salikhov, K., and van der Est, A. (2002) *Mol. Phys.* **100,** 1431–1443
29. Yang, F., Shen, G., Schluchter, W. M., Zybailov, B., Ganago, A. O., Vassiliev,

I. R., Bryant, D. A., and Golbeck, J. H. (1998) *J. Phys. Chem.* **102,** 8288–8299
30. Rigby, S. E., Evans, M. C., and Heathcote, P. (2001) *Biochim. Biophys. Acta* **1507,** 247–259
31. Purton, S., Stevens, D. R., Muhiuddin, I. P., Evans, M. C., Carter, S., Rigby, S. E., and Heathcote, P. (2001) *Biochemistry* **40,** 2167–2175
32. Biggins, J., and Mathis, P. (1988) *Biochemistry* **27,** 1494–1500
33. Malkin, R. (1986) *FEBS Lett.* **208,** 343–346
34. Boudreaux, B., MacMillan, F., Teutloff, C., Agalarov, R., Gu, F., Grimaldi, S., Bittl, R., Brettel, K., and Redding, K. (2001) *J. Biol. Chem.* **276,** 37299–37306
35. Agalarov, R., and Brettel, K. (2003) *Biochim. Biophys. Acta* **1604,** 7–12